


Sensing of Alzheimer's Disease and Multiple Sclerosis Using Nano-Bio Interfaces

Mohammad Javad Hajipour^{a,b,c}, Forough Ghasemi^d, Haniyeh Aghaverdi^b, Mohammad Raoufi^{b,e}, Uwe Linne^f, Fatemeh Atyabi^b, Iraj Nabipour^a, Morteza Azhdarzadeh^b, Hossein Derakhshankhah^g, Alireza Lotfabadi^g, Afshar Bargahi^a, Zahra Alekhamis^b, Afsaneh Aghaie^h, Ehsan Hashemiⁱ.

View metadata, citation and similar papers at core.ac.uk

brought to you by  CORE

provided by Bushehr University of Medical Sciences Repository

^aPersian Gulf Marine Biotechnology Research Center, The Persian Gulf Biomedical Sciences Research Institute, Bushehr University of Medical Sciences, Bushehr, Iran

^bDepartment of Nanotechnology and Nanotechnology Research Center, Faculty of Pharmacy, Tehran University of Medical Sciences, Tehran, Iran

^cNon-Communicable Diseases Research Center, Endocrinology and Metabolism Population Sciences Institute, Tehran University of Medical Sciences, Tehran, Iran

^dDepartment of Chemistry, Sharif University of Technology, Tehran, Iran

^eDepartment of New Materials and Biosystems, Max Planck Institute for Intelligent Systems, Stuttgart, Germany

^fFachbereich Physik/Chemie, Philipps-Universität Marburg, Marburg, Germany

^gDepartment of Pharmaceutical Biomaterials and Medical Biomaterials Research Center, Faculty of Pharmacy, Tehran University of Medical Sciences, Tehran, Iran

^hBlood Transfusion Research Center, High Institute for Research and Education in Transfusion Medicine, Tehran, Iran

ⁱNational Research Center for Transgenic Mouse, National Institute of Genetic Engineering and Biotechnology, Tehran, Iran

^jIranian Center of Neurological Research, Tehran University of Medical Sciences, Tehran, Iran

^kRoozbeh Hospital, Tehran University of Medical Sciences, Tehran, Iran

^lDepartment of Anatomy and Cell Biology and Facility for Electron Microscopy Research, McGill University, Montréal, QC, Canada

Accepted 9 June 2017

Abstract. It is well understood that patients with different diseases may have a variety of specific proteins (e.g., type, amount, and configuration) in their plasmas. When nanoparticles (NPs) are exposed to these plasmas, the resulting coronas may incorporate some of the disease-specific proteins. Using gold (Au) NPs with different surface properties and corona composition, we have developed a technology for the discrimination and detection of two neurodegenerative diseases, Alzheimer's disease (AD) and multiple sclerosis (MS). Applying a variety of techniques, including UV-visible spectra, colorimetric response analyses and liquid chromatography-tandem mass spectrometry, we found the corona-NP complexes, obtained from different human serums, had distinct protein composition, including some specific proteins that are known as AD and MS biomarkers. The colorimetric responses, analyzed by chemometrics and statistical methods, demonstrate

*Correspondence to: Hojatollah Vali, Department of Anatomy and Cell Biology and Facility for Electron Microscopy Research, McGill University, Montréal, QC, H3A 0C7, Canada. E-mail: hojatollah.vali@mcgill.ca and Morteza Mahmoudi, Department

of Nanotechnology and Nanotechnology Research Center, Faculty of Pharmacy, Tehran University of Medical Sciences, Tehran, 13169-43551, Iran. E-mail: mahmoudi-m@tums.ac.ir.

promising capabilities of the technology to unambiguously identify and discriminate AD and MS. The developed colorimetric technology might enable a simple, inexpensive and rapid detection/discrimination of neurodegenerative diseases.

Keywords: Alzheimer's disease, colorimetric technology, disease-specific protein corona, gold nanoparticles, multiple sclerosis

INTRODUCTION

Exposure of nanoparticles (NPs) to physiological fluids results in their surfaces being covered by a biomolecular layer described as a "protein corona" [1–4]. The corona layer gives NPs a different identity compared to their original surface characteristics that will interact with biological systems in a specific way. The composition of the corona defines the bio-distribution, circulation half-life, toxicity and therapeutic efficacy of NPs [5–8]. Therefore, deep understanding of the protein corona composition is crucial to predict the outcome of NPs *in vivo* [9].

Slight variations in the corona composition and structure can induce substantial differences in the biological fate of NPs [7, 10]. For instance, incorporation of apolipoprotein E into the corona composition can enable NPs to cross the blood-brain barrier (BBB) and reach brain tissue [11]. Recently, our group and others have demonstrated that changes in plasma composition, mediated by the type of disease, may be detected in the protein corona of exposed NPs [12–14]. This suggests patients with specific types of diseases have distinct corona composition termed "disease-specific protein corona" (DSPC) [12]. It has been proposed that the formation of the DSPC for different diseases is a consequence of the conformation, concentration, and function of the types of proteins in human plasma/serum. For example, patients with Alzheimer's disease (AD) experience higher levels of the serum amyloid protein, clusterin, Alpha-1-antichymotrypsin, complement factor H and α -1/ β -2-microglobulin with less Apo C3, transthyretin, A β 42:A β 40 ratios and complement C4 compared to normal cases [15–20]. As another example, changing concentrations of anti-myelin antibodies, Epstein-Barr virus, interferon β -neutralizing antibodies, and tumor necrosis factor-related apoptosis-inducing ligand are serum biomarkers in multiple sclerosis (MS) patients [21–23]. In addition, the proteins involved in blood clotting, influence lipid transport pathways leading to a change in the composition of the serum of MS patients, especially in the early stages the disease [24]. These disease-specific serum changes can be used as potential biomarkers at the early stages,

before appearance of any physical characteristic sign for MS disease. The A β oligomer species (A β Os) are known as biomarkers that appear in initial phases of AD [25].

Small variations in the composition of plasma can make significant changes in the corona composition on the surfaces of the same NPs [26]. One could expect, therefore, that the DSPC may be used as a tool to discriminate and/or detect different types of diseases by investigating the plasma of patients with particular diseases. The development of diagnostic approaches for the identification and discrimination of diseases is one of the major challenges facing the scientific community. A major obstacle in disease detection is the clinical symptoms of some diseases, such as fibrillation-related disorders, cancer and MS, only appear at the late stages [27–30]. Currently, a patient's serum and cerebrospinal fluid (CSF) are used to discover new biomarkers (e.g., proteins, metabolites, and macromolecules). Disease-specific biomarkers (e.g., proteins and metabolites) are mainly identified using liquid chromatography-tandem mass spectrometry (LC-MS/MS). Madasamy's group identified several AD biomarkers using flow cytometer-based approaches [31–38]. The analysis of whole proteome and metabolome profiles of patient's serum/cerebrospinal fluid are, however, invasive, time consuming and expensive. In addition, analytical techniques used for these analyses have moderate sensitivity.

Among the various type of sensors, the colorimetric technology is recognized as a rapid, economical, and concise approach for the detection of a wide range of compounds (e.g., biomolecules, environmental pollution compounds like NPs, toxic gases, heavy metals, and toxic industrial chemicals) [39–42]. Array-based detection works on the basis of cross-reactive interactions of different dyes with an analyte leading to the formation of specific colorimetric patterns. Although there is no specific interaction between a dye and analyte, the cross-reactive interactions of dye with sensor elements can provide a unique pattern for the desired analyte [43]. This approach is mimicked from the human mammalian olfactory system for the sense of smell [44]. In this paper, we describe the design and application of a colorimetric technology for the

detection and discrimination of AD and MS. The system consists of four elements of spherical gold (Au) NPs of the same size but with different surface coatings including citrate, cysteine, cysteamine, and polyethyleneglycole. The Au NPs were incubated with 10% and 100% serums obtained from patients with different diseases. The system responses were measured by UV-visible spectra and analyzed by hierarchical cluster analysis (HCA), principal component analysis (PCA), and colorimetric different profile (CDP). Variation in the composition of the protein corona at the surfaces of Au NPs can change their surface plasmon resonance (SPR), which is the basis of sensing in the proposed technique. We have also probed the composition of the protein corona at the surfaces of various NPs obtained from the plasma of patients with different diseases using LC-MS/MS. Serum proteins have low binding affinity to NPs functionalized with zwitterions (Cystein) and therefore lower numbers of proteins, compared to other NPs, can be adsorbed to the surface of these NPs [45]. In this study, we identified the proteins present in the hard corona of citrate/cysteamine/polyethyleneglycole functionalized NPs.

MATERIALS AND METHODS

Materials

L-Cysteamine, sodium citrate, cysteine, thio-sulfate sodium, sodium carbonate, glycine, *Tris* (hydroxymethyl) aminomethane, ammonium persulfate, hydrochloric acid, Sodium chloride, sodium hydrogen phosphate, potassium dihydrogen phosphate and Sodium hydroxide were purchased from Merck. Sodium borohydride, acetic acid, silver nitrate, methanol, ethanol, formaldehyde, sodium dodecyl sulfate, Tetramethylethylenediamine, 2-mercaptoethanol, glycerol, polyethylene glycol, hydrogen tetrachloroaurate cetyltrimethylammonium bromide, L-ascorbic acid and other materials were purchased from Sigma.

Au NPs synthesis and functionalization with citrate, cysteine, cysteamine and polyethylene glycol

Citrate-stabilized Au NPs were prepared using Turkevich method with slight modification [46]. In order to prepare citrate-coated Au NPs, 5 ml of sodium citrate (38.8 mmol L^{-1}) was added to boiling solution of 50 ml of HAuCl_4 (1.0 mmol L^{-1}) and

stirred for 30 min at 100°C . In the next step, the synthesized Au NPs were cooled and functionalized with cysteine, cysteamine or polyethylene glycol. To this end, Au NPs were treated with each of cysteine ($8 \mu\text{M}$), cysteamine ($2 \mu\text{M}$) and thiolated polyethylene glycol ($10 \mu\text{M}$) at room temperature, for 10 hours at pH 7.4. After 10 h of incubation, the produced cysteine-Au, cysteamine-Au and thiolated polyethylene glycol-Au were collected and purified by triplicate centrifugation (at 13000 g for 10 min) and washing.

Characterization of synthesized Au NPs

The synthesized Au NPs were characterized using UV-Visible spectrophotometer and transmission electron microscopy (TEM). All absorbance analyses were accomplished using a Lambda (PerkinElmer, USA) spectrophotometer at room temperature. The Au NP size and morphology were figure out by Phillips CM200 transmission electron microscope (TEM) equipped with an AMT 2.2 CCD camera at an accelerating voltage of 200 kV.

Serum preparation

Blood samples were collected from all volunteers after signing informed consent. The blood samples collected in clot tubes were allowed to clot at 4°C for 30–60 minute and centrifuged following clot formation at 2500 g for 10 min at 4°C . The serum fractions obtained from same subjects (Patients with same disease) were pooled, divided into aliquots and frozen at -20°C . It should be noted that the sex and age (70–80) matched volunteers were selected for this study.

Preparation of corona-coated citrate/cysteine/cysteamine/polyethylene glycol-Au NP complexes

As slight temperature change affects the protein corona formation, the serums (10% and 100%) from AD, MS and normal cases and functionalized Au NPs were maintained at 37°C for 10 min [47]. In the next step, the functionalized Au NPs were incubated with the serums (10% and 100%) at a final concentration of $100 \mu\text{g ml}^{-1}$ at 37°C for 60 min (Total volume was $500 \mu\text{l}$). Immediately after 60 min, the solutions were centrifuged for 20 min at 14000 g at 15°C to separate the corona-coated NP complexes. Then, the supernatant was gently removed and NP-protein pellet was resuspended in PBS (15°C)

and centrifuged for 15 min at 14000 g at 15°C. The washing step was repeated for three times. The triplicate washing lead to detachment of loosely bound proteins. Finally, the resulted hard corona-coated Au NPs were resuspended in 250 μ l of PBS (1%) and used for further analyses.

Dynamic light scattering (DLS) and zeta potential

Size distribution of corona-coated citrate/cysteine/cysteamine/polyethylene glycol-Au complexes were measured using Malvern PCS-4700 instrument equipped with a 256-channel correlator. The surface charges of these complexes were measured by Malvern Zetasizer 3000 HSA. All of these analyses were performed at 25°C and repeated for three times.

Identification of proteins involved in corona using LC-MS/MS analysis

To investigate the effects of changes of serum composition, caused by different types of diseases, on the composition of hard corona, the functionalized Au NPs were incubated with 10% and 100% serums of AD, MS, and healthy individuals. After removing the excess serum and weakly bounded proteins, so called “soft corona”, the obtained hard corona-Au NP complexes were evaluated using LC-MS/MS analyses. The identity and intensity of the hard corona proteins were determined by LC-MS/MS analysis [Tables 2–7 (see also Supplementary Material: Equation 1 and Supplementary Table 2–7)]. Detailed on the LC-MS/MS procedure is provided in our previous report [48].

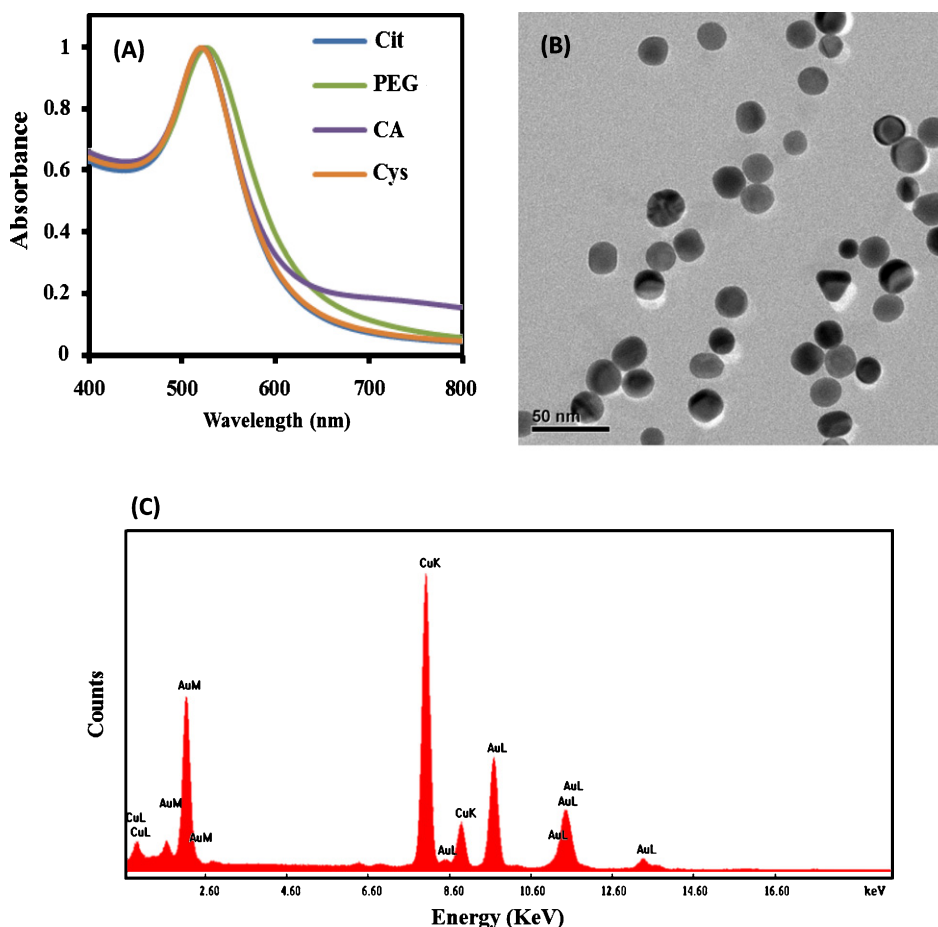


Fig. 1. UV-vis spectra of Au NPs functionalized with citrate, cysteine, cysteamine and polyethyleneglycole (A). Transmission electron microscope (TEM) image of prepared Au NPs (B). Energy dispersive spectroscopy (EDS) analysis of prepared Au NPs (C).

RESULTS AND DISCUSSION

NP synthesis and characterization

The presence of a specific peak at 520 nm confirmed the presence of stable Au NPs in the prepared solutions (Fig. 1A). The UV-visible spectra of citrate/cysteine/cysteamine/polyethylene glycol-coated Au NPs demonstrated no considerable shift in the SPR peak position. On the basis of this result, it is evident the Au NPs have not aggregated in the prepared solutions. Owing to their monodispersed state, the NPs are promising candidates for investigating changes in SPR caused by disease-specific protein coronas (DSPC). Images from transmission electron microscopy (TEM) show sphere-shaped Au NPs (20 nm) with a narrow size distribution (Fig. 1B). Energy dispersive X-ray spectroscopy (EDS) analysis confirmed the presence of pure Au NPs in solution (Fig. 1C).

UV-visible spectra of DSPC-Au NP complexes from different patients

The citrate/cysteine/cysteamine/polyethylene glycol-coated Au NPs were incubated with 10% and 100% serums from various patients and the final DSPC-Au NP complexes measured by UV-visible spectrometry at a wavelength of 400–780 nm. Although the SPRs of all corona-coated Au NP complexes obtained from 10% serums showed no significant shift in peak position, the SPR intensities of some complexes were different from each other (Fig. 2A-D). For example, all corona-coated Au NPs complexes obtained from serums of healthy individuals showed the least SPR intensity except for corona-coated citrate-NPs, which showed the highest intensity (Fig. 2A-D). The SPR intensities of complexes obtained from serums of AD and MS patients were similar (Figs. 2B,D). However, the DSPC-Au NP complexes obtained from 10%

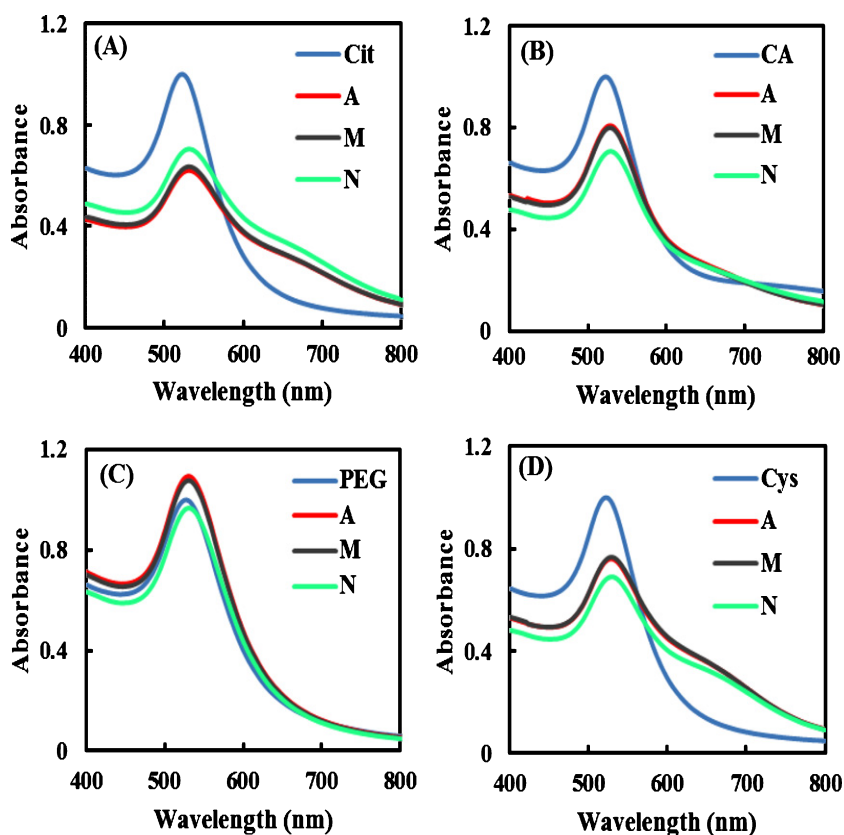


Fig. 2. UV-vis spectra of corona-coated citrate-Au NPs (A), corona-coated cysteamine-Au NPs (B), corona-coated polyethyleneglycol-Au NPs (C) and corona-coated cysteine-Au NPs (D) obtained following incubation with 10% serums of normal, AD and MS cases.

serums can be used to discriminate between healthy individuals and AD/MS patients. It should be noted that these complexes do not discriminate between different diseases. For DSPC-NP complexes from 100% serums, changes in SPR intensity, and in some cases, peak broadening, were observed (Fig. 3A-D). According to the spectral responses recorded for corona-coated citrate-Au NP complexes, distinctive spectra are characteristic for AD and MS (Fig. 3A). As a result of DSPC formation, distinct spectral response permits the facile and rapid detection and discrimination of AD and MS. The different spectral patterns suggest the coronas have a different protein composition.

Analysis of the array responses by hierarchical cluster analysis, principal component analysis and color difference profile

In the method of HCA, different diseases are clustered on the basis of their spatial distances and the results plotted on a dendrogram. The HCA dendrogram represents a view of data clustering in which the

cluster distance is known as an index of likeness level of samples [49]. For 10% serum, the HCA dendrogram shows AD and MS have short or insignificant cluster distances while both diseases have long cluster distances to healthy individuals (Fig. 4A). On the basis of the HCA dendrogram for 100% serum, all AD and MS patients and healthy individuals have long cluster distances from each other (Fig. 4B). The array responses were also analyzed using principal component analysis (PCA) to quantitatively evaluate sample dispersion and determine similarity in the diseases. In the PCA plot, the level of class distribution and separation is known as index of similarity level [50]. In the score plots generated for 10% serum, the horizontal PC1 axis and the vertical PC2 axis captured 96.1% and 3.2% of the variance, respectively (Fig. 5A). As shown in Fig. 5A, the healthy samples can just be discriminated from the disease cases. Indeed, the degree of class separation among different diseases were insignificant, and hence, they cannot be discriminated from each other. In the score plot designed for 100% serum, the horizontal PC1 axis and the vertical PC2 axis captured 93.2% and 5.4% of the variance,

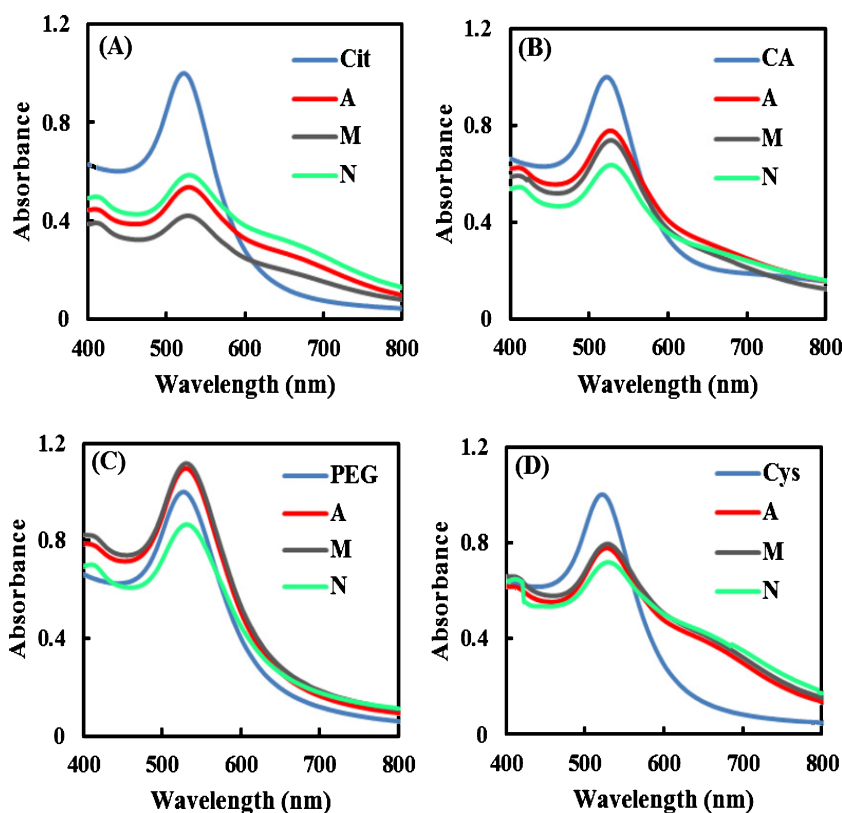


Fig. 3. UV-vis spectra of corona-coated citrate-Au NPs (A), corona-coated cysteamine-Au NPs (B), corona-coated polyethyleneglycole-Au NPs (C) and corona-coated cysteine-Au NPs (D) obtained following incubation with 100% serums of normal, AD and MS cases.

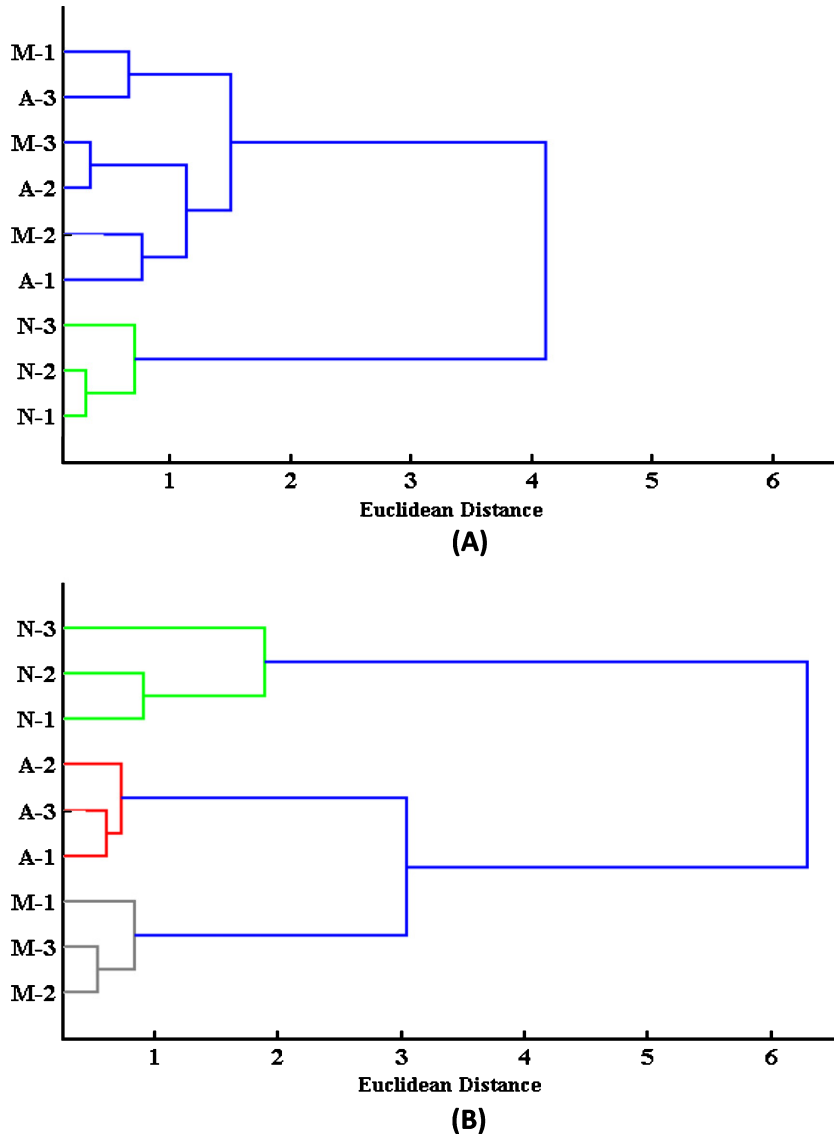


Fig. 4. HCA dendrogram showing the Euclidean distance among different clusters for corona profiles of 10% serum (A) and 100% serum (B).

respectively (Fig. 5B). For 100% serum, all cases can be discriminated from each other. The degree of class separation among AD, MS and healthy individuals were significant, and hence, they can be differentiated (Fig. 5B). These findings can be explained by disease-specific changes in the serum mediated by the disease. Because the colorimetric technology developed in this study differentiate diseases on the basis of the spectral variations driven by DSPCs, they can specifically discriminate patients who have specific protein coronas. In order to differentiate various diseases, even at a glance, CDP was generated by taking the value of the ΔA of three selected visible wave-

lengths (i.e., 520, 570 and 630 nm). CDP provided clear color changes that can be distinguished at a glance. On the basis of the CDP for 10% serum, it is possible to differentiate the healthy case from disease (Fig. 6A). The color changes detected for normal cases may be related to their different SPR intensities. According to the CDP for 100% serum, all cases (AD, MS and healthy) can be distinguished from each other (Fig. 6B). The analysis of the collective array responses by HCA, PCA and CDP suggest DSPC formation can be used to develop colorimetric sensor arrays that specifically discriminate and detect different diseases.

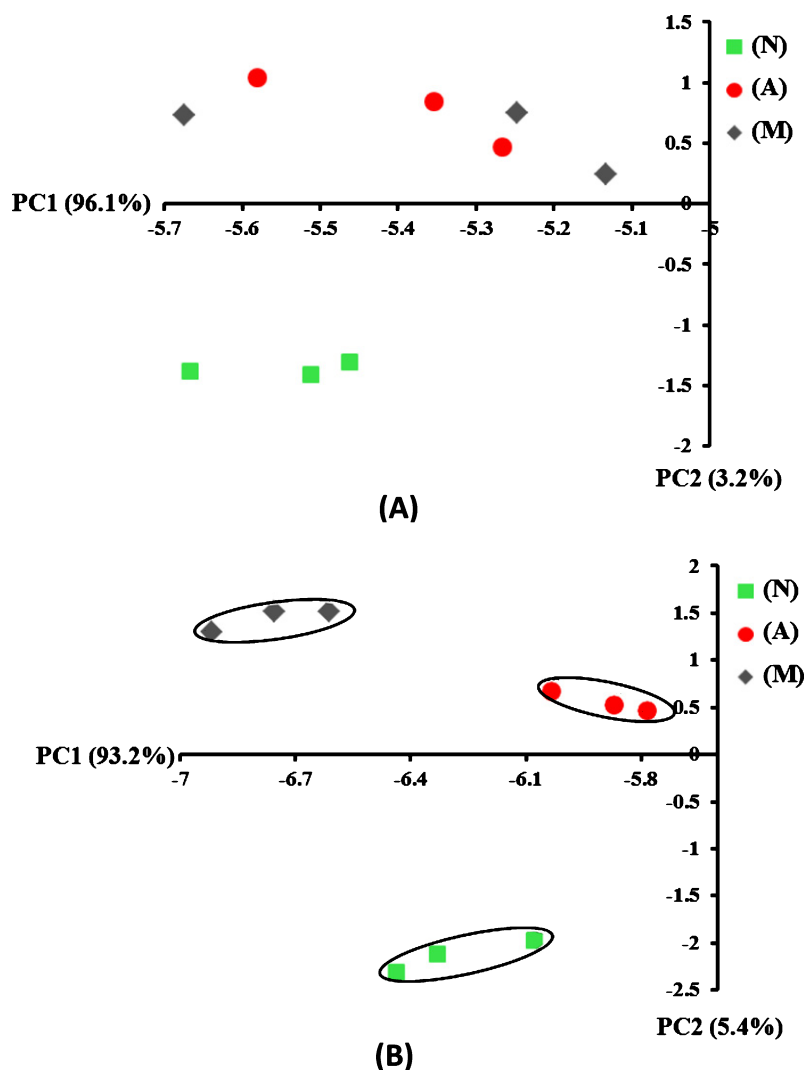


Fig. 5. Two-dimensional score plot showing degree of class separation among normal, AD and MS cases for 10% serum (A) and 100% serum (B).

Size and charge of corona-coated NP complexes

Considering that the size and surface charge of corona-coated NPs are contingent upon the type and affinity of the adsorbed proteins [12], the same NPs will have different properties after exposure to the serum of different patients. Analysis of the size distribution and zeta potential value of corona-coated Au NPs obtained from serums of various patients confirmed this behavior (Tables 1A-D). These results are consistent with previous studies showing personalized protein corona from various patients have distinct size and surface charge [12, 26].

Effects of serum composition on protein corona formation in patients with different diseases

The identified proteins were classified based on their association within different coronas. We found that many proteins (conserved proteins) associated within all coronas (Supplementary Tables 1–6), while some specific proteins exclusively appeared and/or disappeared in hard coronas obtained from particular type of serums (Tables 2–7). In addition, the majority of conserved proteins differently associated within various coronas. These results suggest coronas formed on the surfaces of NPs exposed to serum of

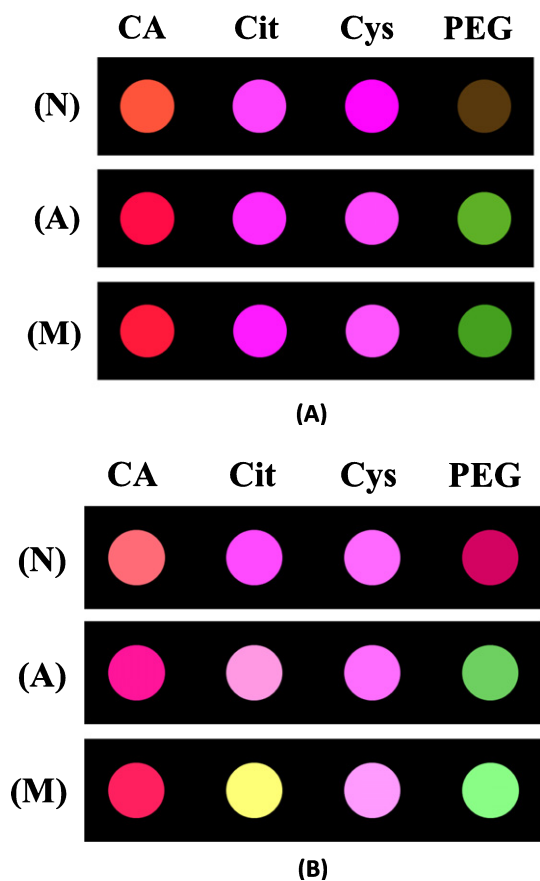


Fig. 6. Color difference profile for normal, AD and MS cases for 10% serum (A) and 100% serum (B).

patients with various diseases are different in terms of the composition and concentration (Tables 2–7, Supplementary Tables 1–6). The conserved proteins (e.g., serum albumin, immunoglobulin, apolipoproteins, and complement factors) showed more association within the protein corona compared to specific proteins (Supplementary Tables 1–6). For citrate-coated NPs, the coronas obtained from 10% serums (diluted in PBS) showed more similarity in their protein pattern compared to those obtained from 100% serums (Supplementary Table 1A,B). Similar results were also observed for PEG-coated NPs (Supplementary Table 3A,B). Interestingly, some proteins were specifically detected in the coronas of both AD and MS. These proteins may help to distinguish patients from normal cases. In the case of cysteamine-coated NPs, apolipoproteins and platelet basic protein seem to be the main component of the hard coronas of both AD and MS (Supplementary Table 2A,B).

Specific proteins identified in the coronas obtained from the serum of patients with a particular disease can be considered as biomarkers predicting disease prevalence and risk (Tables 2–7). Interestingly, some serum proteins that are known as AD and/or MS biomarkers were specifically detected in hard coronas obtained from serums of AD and/or MS diseases. For example, Insulin-like growth factor-binding protein 3, gelsolin, antithrombin, clusterin, Thrombospondin-1 and platelet-basic, which are known as MS biomarkers [51–53], were detected in hard coronas obtained from serums of patients with MS diseases. In addition, AD-specific biomarkers such as Serum amyloid P, complement factor H, Alpha-2-macroglobulin, transthyretin, clusterin, tau-tubulin kinase, Alpha-1-antichymotrypsin, Apolipoprotein B100 and gelsolin were identified in coronas obtained from serums of AD patients [48, 54–57].

Insulin-like growth factor-binding protein 3, gelsolin, antithrombin and clusterin, as MS biomarkers, were only recognized in the corona of cysteamine-NP obtained from 10% serum of MS patients (Table 5). The MS-specific biomarkers such as Thrombospondin-1 and platelet-basic protein were identified in the corona of citrate-NPs obtained from 100% serum of MS patients (Table 2). Serum amyloid P and complement factor H, as AD biomarkers, were recognized in the corona of cysteamine-NPs obtained after incubation with 100% serum of AD patients (Table 4). Alpha-2-macroglobulin, transthyretin, clusterin, and tau-tubulin kinase, as AD biomarkers, were only detected in the corona of citrate-NPs obtained from 10% serum of patients with AD (Table 3). Apolipoprotein B100 and gelsolin, as AD biomarkers, were specifically identified in the coronas of PEG-NPs obtained from 100% and 10% serums of AD patients respectively (Tables 6 and 7). Alpha-1-antichymotrypsin, as AD biomarker, was only identified in the corona of citrate-NPs obtained from 100% serum of AD patients (Table 2). This hard corona complex also had the least amount of apolipoprotein E compared to those obtained from other serums. These results are in agreement with previous studies showing a decrease in the concentration of serum apolipoprotein E in patients with AD [58].

The results of this study are in line with other studies showing that each patient may have a disease-specific protein corona [59, 60]. Every change in serum protein concentration and structure may affect the affinity of proteins toward the NPs and protein

Table 1

DLS and zeta potential values of corona-coated citrate-Au NPs (A), corona-coated cysteamine-Au NPs (B), corona-coated polyethyleneglycole-Au NPs (C) and corona-coated cysteine-Au NPs (D) obtained from 10% and 100% serums of normal, AD and MS cases

A				
Protein corona-coated citrate-Au NPs obtained from normal/patient	DLS serum 10% (nm)	Zeta serum 10% (mV)	DLS serum 100% (nm)	Zeta serum 100% (mV)
Normal	53 ± 09	-9	41 ± 07	-9
Alzheimer's disease	67 ± 05	-9	83 ± 22	-11
Multi sclerosis	51 ± 04	-8	59 ± 10	-6
B				
Protein corona-coated cysteamine-Au NPs obtained from normal/patient	DLS serum 10% (nm)	Zeta serum 10% (mV)	DLS serum 100% (nm)	Zeta serum 100% (mV)
Normal	37 ± 09	-9	65 ± 11	-10
Alzheimer's disease	62 ± 07	-8	43 ± 10	-7
Multi sclerosis	59 ± 05	-4	85 ± 08	-6
C				
Protein corona-coated PEG-Au NPs obtained from normal/patient	DLS serum 10% (nm)	Zeta serum 10% (mV)	DLS serum 100% (nm)	Zeta serum 100% (mV)
Normal	88 ± 15	-8	127 ± 24	-8
Alzheimer's disease	56 ± 04	-3	164 ± 21	-5
Multi sclerosis	81 ± 08	-7	68 ± 15	-6
D				
Protein corona-coated cysteine-Au NPs obtained from normal/patient	DLS serum 10% (nm)	Zeta serum 10% (mV)	DLS serum 100% (nm)	Zeta serum 100% (mV)
Normal	59 ± 13	-3	77 ± 14	-6
Alzheimer's disease	47 ± 10	-5	60 ± 12	-4
Multi sclerosis	69 ± 16	-7	87 ± 08	-10

Table 2

Proteins only detected in the coronas of citrate-NPs obtained from 100% serums of AD and MS patients

Protein identity	NSpC	Protein identity	NSpC
(Corona coated Citrate-NPs obtained after incubation with 100% serum of AD cases)		(Corona coated Citrate-NPs obtained after incubation with 100% serum of MS cases)	
Apolipoprotein B-100	0.961888	Ketohexokinase	0.632403
Protein APOC4-APOC2	2.603969	Histone-lysine N-methyltransferase	0.061802
Ig heavy chain V-I region 5	2.04232	Disintegrin and metalloproteinase domain-containing protein 12	0.206624
Protein SAA2-SAA4	2.235544	ATP-binding cassette sub-family C member 11	0.133295
Alpha-1-antichymotrypsin	0.547795	Complement C1q subcomponent subunit C	0.798011
Trinucleotide repeat-containing gene 6B protein	0.134548	Sickle tail protein homolog	0.096056
Tetrapeptide repeat protein 6	0.1206	Thrombospondin-1	0.158966
Exonuclease 3'-5' domain-containing protein 2	0.371033	Ig heavy chain V-III region POM	1.587822
Ras-related protein Rab-28	1.050776	Protein IGKV1-33	1.736743
Mitogen-activated protein kinase kinase kinase 4	0.143672	Myosin-9	0.090791
Supervillin	0.105361	Complement factor H	0.147868
RING finger protein 225	0.750325	Ig kappa chain V-II region RPMI 6410	1.398541
Nuclear pore complex protein Nup205	0.114527	Ig mu chain C region	2.817381
G-rich sequence factor 1	0.491337	Ig kappa chain V-IV region Len	1.627166
Aryl hydrocarbon receptor repressor	0.342271	Ig heavy chain V-III region BRO	1.555028
		Immunoglobulin lambda-like polypeptide 5	1.776829
		Apolipoprotein A-IV	1.359086
		Alpha-1-acid glycoprotein 1	0.874765
		Antithrombin-III	0.390998
		Ig lambda chain V-IV region Hil	1.785783
		Immunoglobulin J chain	1.136416
		Ig kappa chain V-III region SIE	1.746631
		Hemoglobin subunit beta	2.571223
		Platelet basic protein	2.960657

Table 3
Proteins only detected in the coronas of citrate-NPs obtained from 10% serums of AD and MS patients

Protein identity	NSpC	Protein identity	NSpC
(Corona coated Citrate-NPs obtained after incubation with 10% serum of AD cases)		(Corona coated Citrate-NPs obtained after incubation with 10% serum of MS cases)	
Clusterin	0.44663	Ig kappa chain V-III region SIE	2.554525
Protein FAM65C	0.22268	Apolipoprotein A-IV	0.662574
Protein APOC4-APOC2	1.16944	Apolipoprotein B-100	0.05834
Haptoglobin	0.47746	Ig heavy chain V-III region POM	2.32226
Ig heavy chain V-I region 5	1.83441	VPS10 domain-containing receptor SorCS2	0.234726
Protein IGKV1-33	1.97979	Immunoglobulin lambda-like polypeptide 5	2.598691
Pigment epithelium-derived factor	0.50625	Apolipoprotein L1	0.684043
Alpha-2,8-sialyltransferase 8F	0.52293		
Integrator complex subunit 11	0.34651		
Transthyretin	1.1638		
Metaxin 1, isoform CRA.b	0.45558		
Tau-tubulin kinase	0.12849		
Piezo-type mechanosensitive ion channel component 1	1.83441		
Alpha-2-macroglobulin	0.14358		
Ig kappa chain V-II region	1.59426		
Ig alpha-1 chain C region	0.62265		
Alpha-2-HS-glycoprotein	0.59489		
C4b-binding protein alpha chain	0.69954		

Table 4
Proteins only detected in the coronas of cysteamine-NPs obtained from 100% serums of AD and MS patients

Protein identity	NSpC	Protein identity	NSpC
(Corona coated cysteamine-NPs obtained after incubation with 100% serum of AD cases)		(Corona coated cysteamine-NPs obtained after incubation with 100% serum of MS cases)	
Coagulation factor XII	0.5714	Protein FAM65C	1.81545
Antithrombin-III	2.94556	Elongation factor Tu, mitochondrial	3.85839
Fibronectin	0.58998	Neurogenic locus notch homolog protein 4	0.91192
Complement factor H-related protein 1	2.05769	Kalirin	0.561772
Apolipoprotein A-IV	0.85322	Phosphatidylinositol 4-kinase alpha	0.807126
Ig lambda-2 chain C regions (Fragment)	6.82738	Dual 3',5'-cyclic-AMP and -GMP phosphodiesterase 11A	1.824797
Ig kappa chain C region	1.48438	Niban-like protein 1	2.271855
Plasma kallikrein (Fragment)	0.50384	Dynein heavy chain 8, axonemal	0.354907
ITIH4 protein	0.37288		
Serum amyloid P-component	1.52581		
Partitioning defective 3 homolog B	0.29235		
N-terminal EF-hand calcium-binding protein 3	1.66386		
Pleckstrin homology domain-containing family O member 1	0.83774		
Paralemmin-1	0.9206		
Protein Hook homolog 1	0.45761		
SURP and G-patch domain-containing protein 2	0.3187		
Transcription factor SOX-18	0.94727		
T-complex protein 1 subunit zeta	0.66757		
Lysine-specific demethylase 5A	0.19789		
Prothrombin	0.55308		
Thrombospondin-1	0.29939		
Transient receptor potential cation channel subfamily V member 3	0.42738		
Nesprin-1	0.03831		
ETS translocation variant 3	0.67955		
T-cell immunoreceptor with Ig and ITIM domains	1.14179		
NKG2D ligand 4	1.286		

Table 5
Proteins only detected in the coronas of cysteamine-NPs obtained from 10% serums of AD and MS patients

Protein identity	NSpC	Protein identity	NSpC
(Corona coated cysteamine-NPs obtained after incubation with 10% serum of AD cases)		(Corona coated cysteamine-NPs obtained after incubation with 10% serum of MS cases)	
Ig kappa chain V-III region WOL	7.628765	Pre-mRNA-splicing factor CWC25 homolog	0.232449
Gelsolin	0.522827	Tyrosine-protein kinase SgK223	0.077132
Ig kappa chain V-III region HAH	6.367611	Glutaredoxin domain-containing cysteine-rich protein 2	0.408032
Coagulation factor XII	0.330468	Probable C-mannosyltransferase DPY19L3	0.13872
Proline-rich protein 11	0.558875	PWWP domain-containing protein MUM1	0.142776
Ig heavy chain V-III region BRO	1.69379	Rhodopsin kinase	0.181672
Pigment epithelium-derived factor	0.483731	Sterile alpha motif domain-containing protein 11	0.15857
F-box/LRR-repeat protein 18	0.253597	ABI gene family member 3	0.295645
p53-induced death domain-containing protein 1	0.224674	Solute carrier family 15 member 2	0.141116
Fibronectin	0.085303	Synaptopodin	0.116028
Aldehyde dehydrogenase, mitochondrial	0.39734	Ig kappa chain V-II region RPMI 6410	0.784746
Puromycin-sensitive aminopeptidase	0.21692	Cytochrome c	0.98232
Cell division cycle 5-like protein	0.242841	Protein IGLV3-27 (Fragment)	0.948706
Group XIA secretory phospholipase A2	1.063436	Immunoglobulin J chain	0.637663
		Ig kappa chain V-I region Kue	0.951681
		Protein IGLV3-19 (Fragment)	0.958323
		Complement C1r subcomponent	0.140932
		Clusterin	0.219847
		Protein TRAV34 (Fragment)	0.925858
		Microtubule-associated serine/threonine-protein kinase 4 (Fragment)	1.540459
		Conserved oligomeric Golgi complex subunit 5	0.124437
		Ig lambda chain V-I region WAH	0.984248
		Cytoplasmic dynein 2 heavy chain 1	0.023427
		Ig kappa chain V-III region B6	0.991866
		Pre-mRNA-processing factor 17	0.189719
		Insulin-like growth factor-binding protein 3	0.364359
		Apolipoprotein L1	0.262439
		Protein IGLV3-21 (Fragment)	0.927273
		Ig gamma-3 chain C region	1.615353
		Protein IGKV1-8	1.734001
		Protein IGKV1-12	1.725268
		Alpha-1-antitrypsin	1.729556
		Complement factor H-related protein 1	1.226112
		Alpha-2-macroglobulin	0.353378
		Complement C1q subcomponent subunit B	1.295696
		Serotransferrin	0.449272
		Protein IGHV3OR16-12 (Fragment)	0.896426
		Ig heavy chain V-I region V35	0.887186
		Haptoglobin	0.510588
		Alpha-2-HS-glycoprotein 1	0.585646
		Antithrombin-III	0.438792
		Ig heavy chain V-I region 5 (Fragment)	1.805906
		Ig lambda chain V-I region BL2	0.850798
		Alpha-1-acid glycoprotein 1	0.981693
		Protein IGHV3-15 (Fragment)	0.892887
		Ig kappa chain V-III region NG9 (Fragment)	2.151356
		Ig heavy chain V-I region Mot	0.849858

replacement events on the NP surface regulated predominantly by the Vroman effect [61]. Therefore, it is possible to detect and discriminate different diseases based on diseases-specific protein corona pattern. NPs may show different colloidal stabilities in physiological fluids depending on the type of protein adsorbed to the surface. For example,

proteins attached to the NP surface may decrease the surface charge and consequently neutralize electrostatic repulsion among NPs [62]. The protein corona may also act as a connector and link NPs to each other [63]. These types of protein coronas may increase NP agglomeration. In contrast, some proteins may increase the stability of NPs via increas-

Table 6
Proteins only detected in the coronas of PEG-NPs obtained from 100% serums of AD and MS patients

Protein identity	NSpC	Protein identity	NSpC
(Corona coated PEG-NPs obtained after incubation with 100% serum of AD cases)		(Corona coated PEG-NPs obtained after incubation with 100% serum of MS cases)	
Apolipoprotein B-100	0.159293	Anoctamin-4	0.32462
Beta-2-glycoprotein 1	0.714875	Interferon regulatory factor 2-binding protein 1	0.586538
Inter-alpha-trypsin inhibitor heavy chain H2	0.257154	Olfactory receptor 52A5	1.006359
CYP11B1 protein	0.420367	Tenomodulin	0.974491
Glutamate receptor-interacting protein 1	0.223631	DCN1-like protein (Fragment)	1.540208
Insulin-like growth factor-binding protein 3	0.864359	Kelch-like protein 11	0.451446
Heat shock protein 105 kDa	0.282637	Dynein heavy chain 2, axonemal	0.071268
Pyruvate carboxylase, mitochondrial	0.211194	Cytochrome b-c1 complex subunit 1, mitochondrial	0.687286
C-C chemokine receptor type 7	0.638576		
Armadillo repeat-containing X-linked protein 5	0.439123		
Coiled-coil domain-containing protein 150	0.212622		
Peripheral-type benzodiazepine receptor-associated protein 1	0.136851		
Ig heavy chain V-I region 5 (Fragment)	2.14205		
Enhancer of filamentation 1	0.294826		
Plexin-B2 (Fragment)	1.043972		
Ubiquilin-4	0.428766		

Table 7
Proteins only detected in the coronas of PEG-NPs obtained from 10% serums of AD and MS patients

Protein identity	NSpC	Protein identity	NSpC
(Corona coated PEG-NPs obtained after incubation with 10% serum of AD cases)		(Corona coated PEG-NPs obtained after incubation with 10% serum of MS cases)	
Ig heavy chain V-I region 5	3.734713	Ig mu chain C region	3.014587
Gelsolin	0.556997	Immunoglobulin lambda-like polypeptide 5	5.133242
N-terminal EF-hand calcium-binding protein 3	2.050352	Proline-rich protein 11	0.988207
Brefeldin A-inhibited guanine nucleotide-exchange protein 3	0.198353	Ninein	0.162846
Serotransferrin	4.285257	Immunoglobulin J chain	2.18873
Alpha-2-HS-glycoprotein	1.211148	Structural maintenance of chromosomes protein 1B	0.275262
Fibrinogen alpha chain	0.502597	Zinc finger protein ZIC 5 2	0.578732
		SEC14-like protein 5	0.501794

ing steric/entropic constancy [64]. Corona-coated Au NP complexes obtained from the serums of patients with different diseases have distinct protein composition and concentration. One may expect Au NPs to show different colloidal stability and agglomeration in different serums and thus exhibit variation in SPR intensity/peak position.

The concentration and structure of proteins involved in the corona play a crucial role in determining the colloidal stability of Au NPs [65, 66]. For example, minor Au NP agglomeration was detected when NPs were incubated at high and low concentrations of hemoglobin (Hb). In contrast, Au NP agglomeration considerably increased when a monolayer of Hb coated the NP surface. In this situation, Hb deactivated the electrostatic repulsion forces and/or connected the particles as a pons [65]. Protein

unfolding can also affect NP colloidal stability. The unfolded Albumin caused Au NP aggregation [66]. Structural integrity and protein intensity of the corona governed colloidal stability of NPs in physiological media.

Conclusion

Changes in serum can accurately reflect the state and stage of disease in patients. It is, therefore, possible to detect disease type/progress on the basis of specific changes in composition of serum. Depending on the type and severity of disease, each patient may have distinct DSPC containing disease-specific biomarkers. Owing to the formation of DSPC, some proteins only appeared or disappeared in the corona of a particular disease and may be considered as a

potential biomarker for indicating or predicting disease prevalence/progress or risk. The DSPC-Au NP complexes obtained from serums of different patients showed distinct array responses. The DSPC-based colorimetric technology fulfills the key requirements of sensitivity, specificity, facility, and affordability required for rapid and efficient diagnosis of diseases. The colorimetric technology developed in this study are able to discriminate and detect AD and MS on the basis of the DSPC. Further developments are, however, needed to improve the specificity and sensitivity of DSPC-based colorimetric technology.

DISCLOSURE STATEMENT

Authors' disclosures available online (<http://j-alz.com/manuscript-disclosures/16-0206r3>).

SUPPLEMENTARY MATERIAL

The supplementary material is available in the electronic version of this article: <http://dx.doi.org/10.3233/JAD-160206>.

REFERENCES

- [1] Lynch I, Dawson KA (2008) Protein-nanoparticle interactions. *Nano Today* **3**, 40-47.
- [2] Cedervall T, Lynch I, Lindman S, Berggård T, Thulin E, Nilsson H, Dawson KA, Linse S (2007) Understanding the nanoparticle-protein corona using methods to quantify exchange rates and affinities of proteins for nanoparticles. *Proc Natl Acad Sci U S A* **104**, 2050-2055.
- [3] Mahmoudi M, Lynch I, Ejtehadi MR, Monopoli MP, Bombelli FB, Laurent S (2011) Protein-nanoparticle interactions: Opportunities and challenges. *Chem Rev* **111**, 5610-5637.
- [4] Del Pino P, Pelaz B, Zhang Q, Maffre P, Nienhaus GU, Parak WJ (2014) Protein corona formation around nanoparticles—from the past to the future. *Mater Horiz* **1**, 301-313.
- [5] Hajipour MJ, Akhavan O, Meidanchi A, Laurent S, Mahmoudi M (2014) Hyperthermia-induced protein corona improves the therapeutic effects of zinc ferrite spinel-graphene sheets against cancer. *RSC Adv* **4**, 62557-62565.
- [6] Monopoli MP, Åberg C, Salvati A, Dawson KA (2012) Biomolecular coronas provide the biological identity of nanosized materials. *Nat Nanotechnol* **7**, 779-786.
- [7] Lynch I, Salvati A, Dawson KA (2009) Protein-nanoparticle interactions: What does the cell see? *Nat Nanotechnol* **4**, 546-547.
- [8] Aggarwal P, Hall JB, McLeland CB, Dobrovolskaia MA, McNeil SE (2009) Nanoparticle interaction with plasma proteins as it relates to particle biodistribution, biocompatibility and therapeutic efficacy. *Adv Drug Deliv Rev* **61**, 428-437.
- [9] Mirshafiee V, Kim R, Park S, Mahmoudi M, Kraft ML (2016) Impact of protein pre-coating on the protein corona composition and nanoparticle cellular uptake. *Biomaterials* **75**, 295-304.
- [10] Tenzer S, Docter D, Kuharev J, Musyanovych A, Fetz V, Hecht R, Schlenk F, Fischer D, Kiouptsi K, Reinhardt C (2013) Rapid formation of plasma protein corona critically affects nanoparticle pathophysiology. *Nat Nanotechnol* **8**, 772-781.
- [11] Mahmoudi M, Sheibani S, Milani AS, Rezaee F, Gauberti M, Dinarvand R, Vali H (2015) Crucial role of the protein corona for the specific targeting of nanoparticles. *Nanomedicine* **10**, 215-226.
- [12] Hajipour MJ, Laurent S, Aghaie A, Rezaee F, Mahmoudi M (2014) Personalized protein coronas: A “key” factor at the nanobiointerface. *Biomater Sci* **2**, 1210-1221.
- [13] Caracciolo G (2015) Liposome-protein corona in a physiological environment: Challenges and opportunities for targeted delivery of nanomedicines. *Nanomedicine* **11**, 543-557.
- [14] Caracciolo G, Caputo D, Pozzi D, Colapicchioni V, Coppola R (2014) Size and charge of nanoparticles following incubation with human plasma of healthy and pancreatic cancer patients. *Colloids Surf B Biointerfaces* **123**, 673-678.
- [15] Hye A, Lynham S, Thambisetty M, Causevic M, Campbell J, Byers H, Hooper C, Rijdsdijk F, Tabrizi S, Banner S (2006) Proteome-based plasma biomarkers for Alzheimer's disease. *Brain* **129**, 3042-3050.
- [16] Song F, Poljak A, Crawford J, Kochan NA, Wen W, Cameron B, Lux O, Brodaty H, Mather K, Smythe GA (2012) Plasma apolipoprotein levels are associated with cognitive status and decline in a community cohort of older individuals. *PLoS One* **7**, e34078.
- [17] Hye A, Riddoch-Contreras J, Baird AL, Ashton NJ, Bazenet C, Leung R, Westman E, Simmons A, Dobson R, Sattler M (2014) Plasma proteins predict conversion to dementia from prodromal disease. *Alzheimers Dement* **10**, 799-807. e792.
- [18] Licastro F, Pedrini S, Davis LJ, Caputo L, Tagliabue J, Savorani G, Cucinotta D, Annoni G (2001) α -1-antichymotrypsin and oxidative stress in the peripheral blood from patients with probable Alzheimer disease: A short-term longitudinal study. *Alzheimer Dis Assoc Disord* **15**, 51-55.
- [19] Liu Y, Qing H, Deng Y (2014) Biomarkers in Alzheimer's disease analysis by mass spectrometry-based proteomics. *Int J Mol Sci* **15**, 7865-7882.
- [20] Llano DA, Devanarayan V, Simon AJ, Alzheimer's Disease Neuroimaging Initiative (ADNI) (2013) Evaluation of plasma proteomic data for Alzheimer disease state classification and for the prediction of progression from mild cognitive impairment to Alzheimer disease. *Alzheimer Dis Assoc Disord* **27**, 233-243.
- [21] Genain CP, Cannella B, Hauser SL, Raine CS (1999) Identification of autoantibodies associated with myelin damage in multiple sclerosis. *Nat Med* **5**, 170-175.
- [22] Boz C, Oger J, Gibbs E, Grossberg S (2007) Reduced effectiveness of long-term interferon- β treatment on relapses in neutralizing antibody-positive multiple sclerosis patients: A Canadian multiple sclerosis clinic-based study. *Mult Scler* **13**, 1127-1137.
- [23] Ascherio A, Munger KL (2007) Environmental risk factors for multiple sclerosis. Part I: The role of infection. *Ann Neurol* **61**, 288-299.

- [24] Wallin M, Oh U, Nyalwidhe J, Semmes J, Kislinger T, Coffman P, Kurtzke J, Jacobson S (2015) Serum proteomic analysis of a pre-symptomatic multiple sclerosis cohort. *Eur J Neurol* **22**, 591-599.
- [25] Benilova I, Karran E, De Strooper B (2012) The toxic A [beta] oligomer and Alzheimer's disease: An emperor in need of clothes. *Nat Neurosci* **15**, 349.
- [26] Hajipour MJ, Raheb J, Akhavan O, Arjmand S, Mashinchian O, Rahman M, Abdolahad M, Serpooshan V, Laurent S, Mahmoudi M (2015) Personalized disease-specific protein corona influences the therapeutic impact of graphene oxide. *Nanoscale* **7**, 8978-8994.
- [27] Nestor PJ, Scheltens P, Hodges JR (2004) Advances in the early detection of Alzheimer's disease. *Nat Rev Neuro* **5**, S34-S41.
- [28] Kuhlmann T, Lingfeld G, Bitsch A, Schuchardt J, Brück W (2002) Acute axonal damage in multiple sclerosis is most extensive in early disease stages and decreases over time. *Brain* **125**, 2202-2212.
- [29] Confavreux C, Vukusic S, Moreau T, Adeleine P (2000) Relapses and progression of disability in multiple sclerosis. *N Engl J Med* **343**, 1430-1438.
- [30] Yachida S, Jones S, Bozic I, Antal T, Leary R, Fu B, Kamiyama M, Hruban RH, Eshleman JR, Nowak MA (2010) Distant metastasis occurs late during the genetic evolution of pancreatic cancer. *Nature* **467**, 1114-1117.
- [31] Petricoin EF, Belluco C, Araujo RP, Liotta LA (2006) The blood peptidome: A higher dimension of information content for cancer biomarker discovery. *Nat Rev Cancer* **6**, 961-967.
- [32] Chen X, Ba Y, Ma L, Cai X, Yin Y, Wang K, Guo J, Zhang Y, Chen J, Guo X (2008) Characterization of microRNAs in serum: A novel class of biomarkers for diagnosis of cancer and other diseases. *Cell Res* **18**, 997-1006.
- [33] Blennow K, Hampel H, Weiner M, Zetterberg H (2010) Cerebrospinal fluid and plasma biomarkers in Alzheimer disease. *Nat Rev Neurol* **6**, 131-144.
- [34] Mapstone M, Cheema AK, Fiandaca MS, Zhong X, Mhyre TR, MacArthur LH, Hall WJ, Fisher SG, Peterson DR, Haley JM (2014) Plasma phospholipids identify antecedent memory impairment in older adults. *Nat Med* **20**, 415-418.
- [35] Viola KL, Sbarboro J, Sureka R, De M, Bicca MA, Wang J, Vasavada S, Satpathy S, Wu S, Joshi H (2015) Towards non-invasive diagnostic imaging of early-stage Alzheimer's disease. *Nat Nanotechnol* **10**, 91-98.
- [36] Madasamy S, Chaudhuri V, Kong R, Alderete B, Adams CM, Knaak TD, Ruan W, Wu AH, Bigos M, Amento EP (2015) Plaque array method and proteomics-based identification of biomarkers from Alzheimer's disease serum. *Clin Chim Acta* **441**, 79-85.
- [37] Guo L-H, Alexopoulos P, Wagenpfeil S, Kurz A, Perneczky R, Alzheimer's Disease Neuroimaging Initiative (2013) Plasma proteomics for the identification of Alzheimer's disease. *Alzheimer Dis Assoc Disord* **27**, 337-342.
- [38] Tremlett H, Dai DL, Hollander Z, Kapanen A, Aziz T, Wilson-McManus JE, Tebbutt SJ, Borchers CH, Oger J, Freue GVC (2015) Serum proteomics in multiple sclerosis disease progression. *J Proteomics* **118**, 2-11.
- [39] Ghasemi F, Hormozi-Nezhad MR, Mahmoudi M (2015) A colorimetric sensor array for detection and discrimination of biothiols based on aggregation of gold nanoparticles. *Anal Chim Acta* **882**, 58-67.
- [40] Lin H, Suslick KS (2010) A colorimetric sensor array for detection of triacetone triperoxide vapor. *J Am Chem Soc* **132**, 15519-15521.
- [41] Feng L, Musto CJ, Kemling JW, Lim SH, Suslick KS (2010) A colorimetric sensor array for identification of toxic gases below permissible exposure limits. *Chem Commun* **46**, 2037-2039.
- [42] Lim SH, Feng L, Kemling JW, Musto CJ, Suslick KS (2009) An optoelectronic nose for the detection of toxic gases. *Nat Chem* **1**, 562-567.
- [43] Askim JR, Mahmoudi M, Suslick KS (2013) Optical sensor arrays for chemical sensing: The optoelectronic nose. *Chem Soc Rev* **42**, 8649-8682.
- [44] Rakow NA, Suslick KS (2000) A colorimetric sensor array for odour visualization. *Nature* **406**, 710-713.
- [45] Mahmoudi M, Bertrand N, Zope H, Farokhzad OC (2016) Emerging understanding of the protein corona at the nano-bio interfaces. *Nano Today* **11**, 817-832.
- [46] Kimling J, Maier M, Okenve B, Kotaidis V, Ballot H, Plech A (2006) Turkevich method for gold nanoparticle synthesis revisited. *J Phys Chem B* **110**, 15700-15707.
- [47] Mahmoudi M, Shokrgozar MA, Behzadi S (2013) Slight temperature changes affect protein affinity and cellular uptake/toxicity of nanoparticles. *Nanoscale* **5**, 3240-3244.
- [48] Bigdeli A, Palchetti S, Pozzi D, Hormozi-Nezhad MR, Baldelli Bombelli F, Caracciolo G, Mahmoudi M (2016) Exploring cellular interactions of liposomes using protein corona fingerprints and physicochemical properties. *ACS Nano* **10**, 3723-3737.
- [49] Almeida J, Barbosa L, Pais A, Formosinho S (2007) Improving hierarchical cluster analysis: A new method with outlier detection and automatic clustering. *Chemometr Intell Lab Syst* **87**, 208-217.
- [50] Bro R, Smilde AK (2014) Principal component analysis. *Anal Methods* **6**, 2812-2831.
- [51] Fiorini A, Koudriavtseva T, Bucaj E, Coccia R, Foppoli C, Giorgi A, Schininà ME, Di Domenico F, De Marco F, Perluigi M (2013) Involvement of oxidative stress in occurrence of relapses in multiple sclerosis: The spectrum of oxidatively modified serum proteins detected by proteomics and redox proteomics analysis. *PLoS One* **8**, e65184.
- [52] Villoslada P (2010) Biomarkers for multiple sclerosis. *Drug News Perspect* **23**, 585-595.
- [53] Tomioka R, Matsui M (2014) Biomarkers for multiple sclerosis. *Intern Med* **53**, 361-365.
- [54] Zabel M, Schrag M, Mueller C, Zhou W, Crofton A, Petersen F, Dickson A, Kirsch WM (2012) Assessing candidate serum biomarkers for Alzheimer's disease: A longitudinal study. *J Alzheimers Dis* **30**, 311-321.
- [55] Han S-H, Jung ES, Sohn J-H, Hong HJ, Hong HS, Kim JW, Na DL, Kim M, Kim H, Ha HJ (2011) Human serum transthyretin levels correlate inversely with Alzheimer's disease. *J Alzheimers Dis* **25**, 77-84.
- [56] Dursun E, Gezen-Ak D, Hanağasi H, Bilgiç B, Lohmann E, Ertan S, Atasoy İL, Alaylioğlu M, Araz ÖS, Önal B (2015) The interleukin 1 alpha, interleukin 1 beta, interleukin 6 and alpha-2-macroglobulin serum levels in patients with early or late onset Alzheimer's disease, mild cognitive impairment or Parkinson's disease. *J Neuroimmunol* **283**, 50-57.
- [57] Doecke JD, Laws SM, Faux NG, Wilson W, Burnham SC, Lam C-P, Mondal A, Bedo J, Bush AI, Brown B (2012) Blood-based protein biomarkers for diagnosis of Alzheimer disease. *Arch Neurol* **69**, 1318-1325.
- [58] Rasmussen KL, Tybjærg-Hansen A, Nordestgaard BG, Frikke-Schmidt R (2015) Plasma levels of apolipoprotein E and risk of dementia in the general population. *Ann Neurol* **77**, 301-311.

- [59] Colapicchioni V, Tilio M, Digiacoimo L, Gambini V, Palchetti S, Marchini C, Pozzi D, Occhipinti S, Amici A, Caracciolo G (2015) Personalized liposome–protein corona in the blood of breast, gastric and pancreatic cancer patients. *Int J Biochem Cell Biol* **75**, 180-187.
- [60] Caputo D, Papi M, Coppola R, Palchetti S, Digiacoimo L, Caracciolo G, Pozzi D (2017) A protein corona-enabled blood test for early cancer detection. *Nanoscale* **9**, 349-354.
- [61] Vroman L (1962) Effect of adsorbed proteins on the wettability of hydrophilic and hydrophobic solids. *Nature* **196**, 476-477.
- [62] Chanana M, Correa-Duarte MA, Liz-Marzán LM (2011) Insulin-coated gold nanoparticles: a plasmonic device for studying metal–protein interactions. *Small* **7**, 2650-2660.
- [63] Bharti B, Meissner J, Findenege GH (2011) Aggregation of silica nanoparticles directed by adsorption of lysozyme. *Langmuir* **27**, 9823-9833.
- [64] Chanana M, Rivera-Gil P, Correa-Duarte MA, Liz-Marzán LM, Parak WJ (2013) Physicochemical properties of protein-coated gold nanoparticles in biological fluids and cells before and after proteolytic digestion. *Angew Chem Int Ed Engl* **52**, 4179-4183.
- [65] Moerz ST, Kraegeloh A, Chanana M, Kraus T (2015) Formation mechanism for stable hybrid clusters of proteins and nanoparticles. *ACS Nano* **9**, 6696-6705.
- [66] Dominguez-Medina S, Kisley L, Tauzin LJ, Hoggard A, Shuang B, DS Indrasekara AS, Chen S, Wang L-Y, Derry PJ, Liopo A (2016) Adsorption and unfolding of a single protein triggers nanoparticle aggregation. *ACS Nano* **10**, 2103-2112.